Materials Science Forum
ISSN: 1662-9752, Vol. 1082, pp 171-176
doi:10.4028/p-884q32

Submitted: 2022-05-27
Revised: 2022-09-05
Accepted: 2023-01-12
Online: 2023-03-31

Comparison of Microstructure and Properties of Nickel-Copper Alloy Prepared by Casting and Laser Powder Bed Fusion Process

Alice Chlupová[1,a*], Ivo Šulák[1,b], Ivo Kuběna[1,c], Tomáš Kruml[1,d], Jan-Philipp Roth[2,e] and Katrin Jahns[2,3,f]

[1]Institute of Physics of Materials, The Czech Academy of Sciences, Žižkova 22, 616 00 Brno, Czech Republic

[2]Laboratory for Materials Design and Structural Integrity, Osnabrück University of Applied Sciences, Albrechtstr. 30, 49076 Osnabrück, Germany

[3]Steel Institute IEHK, RWTH Aachen University, Intzestraße 1, 52072 Aachen, Germany

[a*]chlupova@ipm.cz, [b]sulak@ipm.cz, [c]kubena@ipm.cz, [d]kruml@ipm.cz, [e]j.roth@hs-osnabrueck.de, [f]katrin.jahns@iehk.rwth-aachen.de

Keywords: nickel-copper alloy; microstructure; tensile properties; fractography; casting; laser powder bed fusion.

Abstract. Nickel-copper alloys are commonly used in highly corrosive conditions where strength is required. Typical applications are in the marine sector, petrochemical industry, or energy facilities such as chemical tubes, pumps, heat exchangers and superheated steam systems. This paper compares the microstructure and mechanical properties of a cast alloy with a 3D printed alloy processed via a laser powder bed fusion (LPBF) technique. Small cylindrical specimens were used for tensile tests at room temperature (RT) and elevated temperatures up to 750 °C in air. The tensile stress-strain response was determined for both types of materials. At RT, LPBF material has a higher yield strength and ultimate tensile strength than a cast alloy. At elevated temperatures, the strength of both variants is comparable. However, the fracture elongation of the LPBF material is significantly lower over the entire range of investigated temperatures. Fracture surfaces and polished sections parallel to the specimen axis were investigated to compare the microstructure and damage mechanisms of the nickel-coper alloy 400 prepared by conventional casting and via LPBF.

Introduction

Nickel-copper-based alloys contain usually from 52 to 67 % nickel. The high variability of alloying elements gives rise to materials with a wide range of properties. Alloy 400 (material number 2.4360) is a single phase alloy strengthened by Mn, Si, Fe and C [1]. Alloy 400 is stronger than pure nickel; its high toughness is maintained over a considerable range of temperatures. It also has good ductility and thermal conductivity. It has excellent mechanical properties at subzero temperatures without a ductile-to-brittle transition. It exhibits relatively low hardness between 115 and 250 HV which excludes this material from applications exposed to adhesive wear, erosion, or cavitation. Alloy 400 offers exceptional resistance to corrosion by many aggressive agents, i.e. hydrofluoric, sulfuric and hydrochloric acids and rapidly flowing seawater. It is commonly used in highly corrosive conditions in applications where strength is needed as pumps in marine engineering, heat exchangers and condenser tubes in the chemical industry and superheated steam systems in power applications [2, 3].

Additive manufacturing (AM) has developed significantly in recent years. It can be used not only for the improvement of functionality and weight reduction of complex-shape components that are difficult to produce by conventional machining but also for maintenance and repair operations [4]. With the evolvement of AM and a price reduction for 3D printers, the possibilities to create functional end-use components not only from plastics but also from metals have been expanded [5]. As additive manufacturing becomes more feasible, there is a growing need to increase knowledge of the microstructure and associated mechanical properties of 3D printed metallic materials. Laser powder bed fusion (LPBF) is an AM process where a laser is used as a heat source to fuse powder feedstock

to create a 3D object [4]. Lasers are widely used in metal processing due to their ability to deliver high power focused in a precise spot and quickly heat the material. This feature makes the laser a perfect device for obtaining specific properties in metals due to microstructural modification. Moreover, another advantage can be seen in changes in chemical composition if additional material is supplied to the molten pool, e.g. oxides to obtain the ODS version of the material [6].

The work is aimed to compare the microstructure and fracture mode of the Alloy 400 prepared either conventionally by casting or unconventionally by the LPBF method. The effect of microstructure on mechanical properties and appearance of the fracture under mechanical loading was monitored and discussed in terms of material production way.

Experiment

The chemical composition of the Alloy 400 alloy according to DIN 17743 is listed in Table 1. Two types of materials were studied, i.e. cast and prepared by LPBF. Microstructural analysis was performed on the cross-sectional metallographic samples prepared by grinding with SiC papers and polishing with silica suspensions. Both cast and LPBF materials were characterized by scanning electron microscopy (SEM) using TESCAN LYRA 3 XMU FEG/SEM x FIB. Grain size and orientation were characterized using electron backscatter diffraction (EBSD). The EBSD data were acquired using an Oxford Symmetry EBSD detector with an Aztec control system. To determine the mechanical properties of the two types of Alloy 400, cylindrical specimens with a gauge length of 9 mm and diameter of 3 mm were used. Specimens were machined at IPM; the specimen axis for the LPBF variant was perpendicular to the building direction. Tensile tests were performed until a complete fracture using a universal test system (Instron 8862) with an electromechanical actuator at a cross-head displacement rate of 1 mm/min. The morphology of the fracture surfaces was observed using SEM to analyse the failure mechanisms.

Table 1 Chemical composition of Alloy 400 [wt. %]

Cu	Fe	Mn	Si	Al	C	Ni
28 – 34	1.0 – 2.5	2.0 max	0.5 max	0.5 max	0.15 max	63 min

Results and Discussion

The microstructure of Alloy 400 prepared by two different methods, i.e. conventional casting and LPBF is presented in Fig. 1. The microstructure of the cast variant is composed of equiaxed grains with the presence of twins typical for cast material (Fig. 1a). The grain orientation map in the Z direction is shown in Fig. 1b and it revealed the random grain orientation. The microstructure of LPBF material is composed of cells / melting pools typical for materials prepared by this type of AM (Fig. 1c). The material exhibits preferential <110> orientation in the building direction and random orientation in the perpendicular directions (see Fig. 1d).

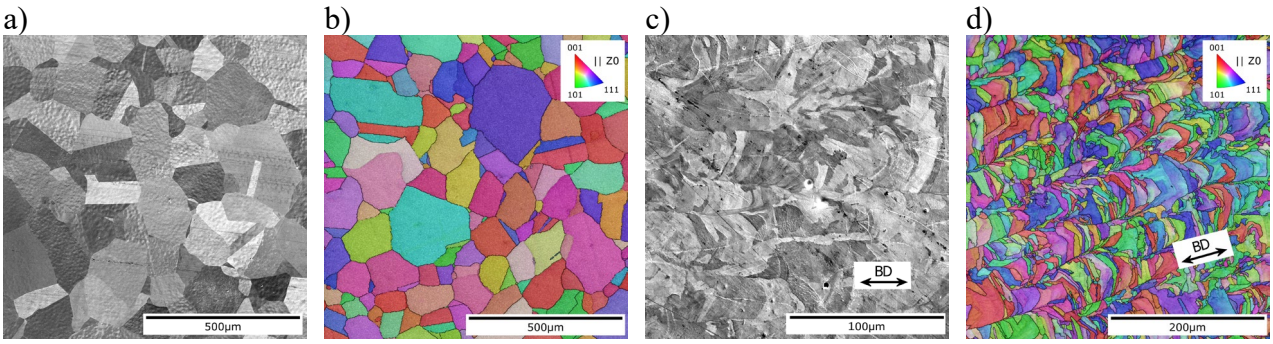

Fig. 1 SEM micrographs and EBSD maps for the cast (a,b) and LPBF variant (c,d) of Alloy 400.

Contrary to the conventionally prepared material, no twins were detected. The average grain size of both material variants as obtained from EBSD data post-processing is: cast = 63 ± 49 μm (excluding twin boundaries), LPBF = 16 ± 11 μm. The density of the LPBF variant was evaluated from metallographic sections to 99.5 %.

Tensile properties were evaluated up to 750 °C and results are plotted in Fig. 2. For comparable temperatures, higher values of yield and ultimate tensile strength exhibited the LPBF variant of Alloy 400, nevertheless, the plasticity decreased. These results are supported by the findings of Raffeis [7]. The higher strength can be ascribed to the significant refinement of the microstructure. However, contrary to the result in [7] the fracture elongation is lower, which can be explained by the presence of defects in the LPBF variant of material as was confirmed by fractography analysis.

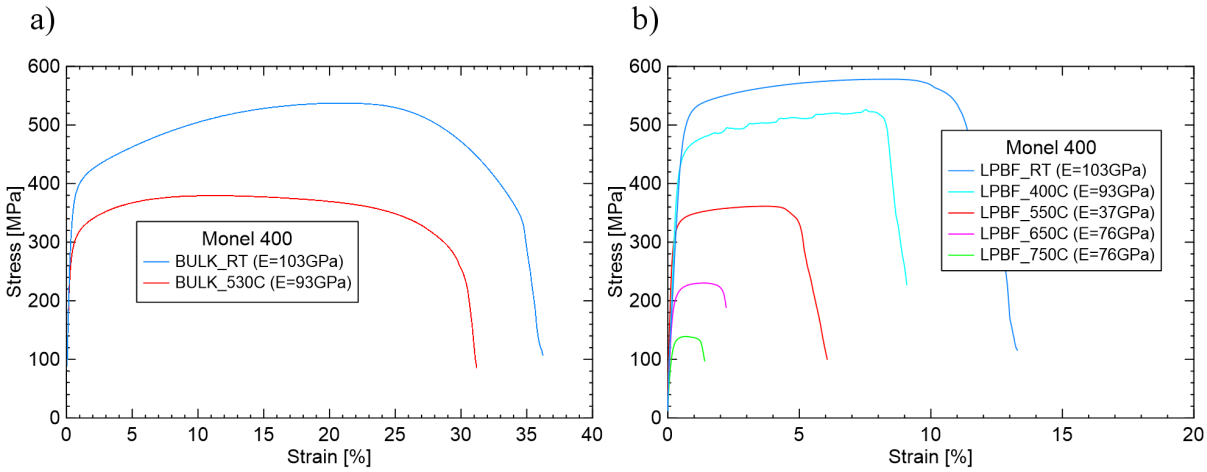

Fig. 2 Tensile properties: cast (a) and LPBF variant (b) of Alloy 400 at different temperatures.

Fracture surfaces of the specimens tested at two temperatures were selected for fractographical observation (Fig. 3). Initial visual investigation revealed high plasticity accompanied by strong necking in the case of cast material. The fracture surface was rough with significant height differences. In comparison with that, fracture surfaces of specimens prepared by LPBF exhibited small height differences, i.e. the fracture surface was relatively flat and part of the fracture consisted of pores arranged in rows. The lower plasticity was confirmed by weak necking of specimens before fracture, nevertheless, the dimples typically associated with ductile fracture were observed at higher magnification.

Results of detailed observation of typical patterns present on a fracture surface of the tensile specimen of cast variant tested at RT are shown in Fig. 4. The micrograph in Fig 4a shows typical ductile dimples. In Fig. 4b, there are wrinkles present on the cylindrical part of gauge length resulting from strong plastic deformation in the area of necking. Similar features were observed for a cast specimen tested at 530 °C where slightly smaller ductile dimples were observed and additional features in the form of oxide layer were present.

Analogically to the cast specimen, the thorough analysis of typical fractography patterns on the fractured specimen from LPBF material was performed and results for the specimen tested at RT are shown in Fig. 5. In comparison with the cast variant, the necking is weak and the whole fracture surface exhibits quite low height differences (see overview in Fig. 5a). The fracture surface consists of mainly two patterns: bands of large pores (keyholes) arranged in rows (see Fig. 5b) and a slightly dimpled surface (see Fig. 5c). The cylindrical part of the LPBF specimen shows a flat surface. It is important to note that the surface was post-processed and it does not show an outer surface processed by LPBF. Similar features on the fracture surface were observed in the case of the LPBF specimen tested at 550 °C. Except for ductile dimples and the bands of keyhole porosity also the occasional presence of „cleavage-like“ facets was observed. It confirms the lower plasticity in comparison with the specimen tested at RT (see the plot in Fig. 2b where fracture elongation decreases from 13 % at RT to 6 % at 550 °C).

The formation of internal defects depends strongly on the applied processing conditions and set up parameters so they can be seen as a particular process fingerprint. Different pore sizes, shapes, and distributions result in different stress concentrations and stimulate the initiation and propagation of cracks differently. No casting defects were observed on the fracture surface of cast specimens of Alloy 400, nevertheless, the LPBF variant of material exhibited the occurrence of printing defects. In [8], a comprehensive description of the formation of pores during the LPBF process was published concerning process parameters such as laser power, distance of melt pools, powder layer thickness, scanning speed, scanning strategy, powder properties, inert gas, etc. and three types of defects were described: 1) lack-of-fusion defects (LOF), 2) gas porosity and 3) balling.

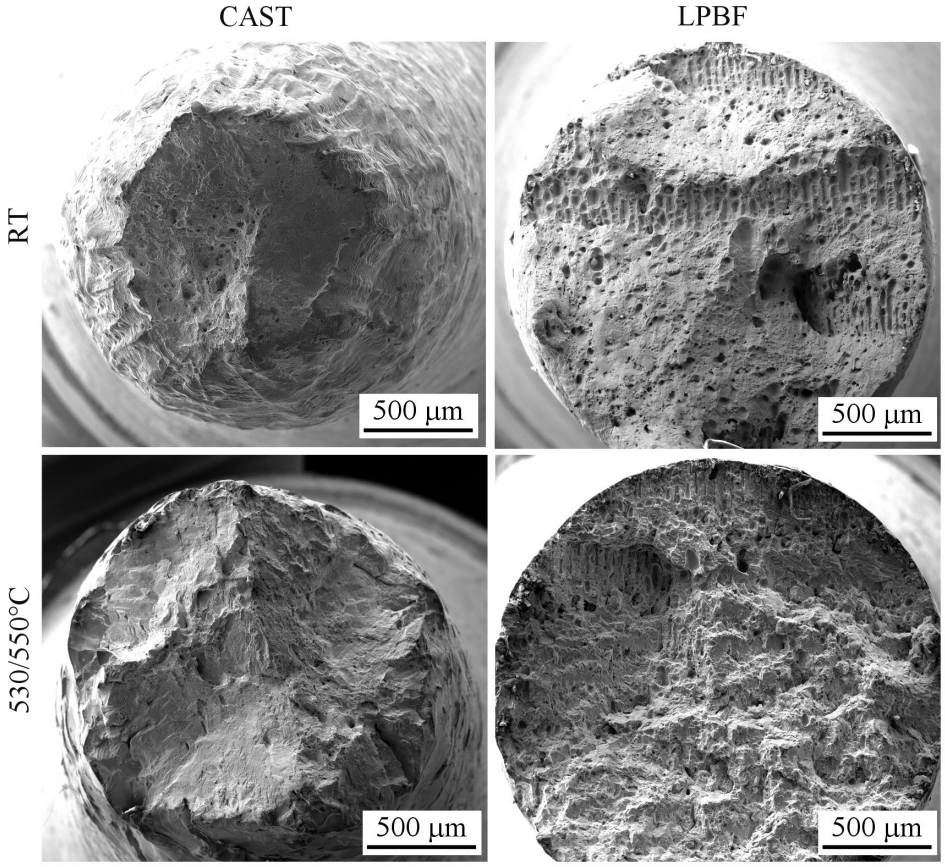

Fig. 3 Micrographs of fracture surfaces of tensile specimens for the cast (left) and LPBF variant (right) of Alloy 400 at RT (up) and elevated temperature 530/550 °C (down).

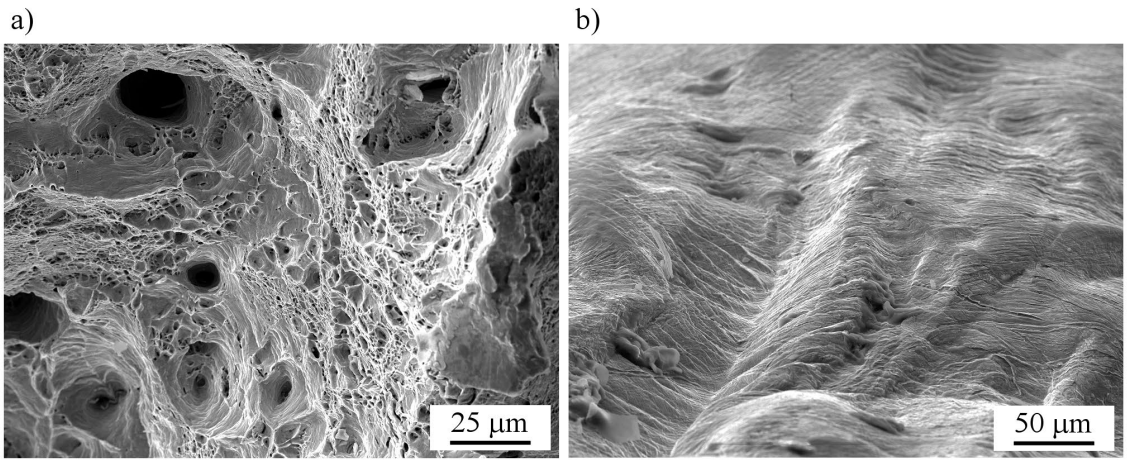

Fig. 4 Detail of fracture surface of tensile specimens for the cast variant at RT. Typical ductile dimples on fracture surface (a) and wrinkles on the cylindrical part of specimen resulting from strong plastic deformation in the area of necking (b).

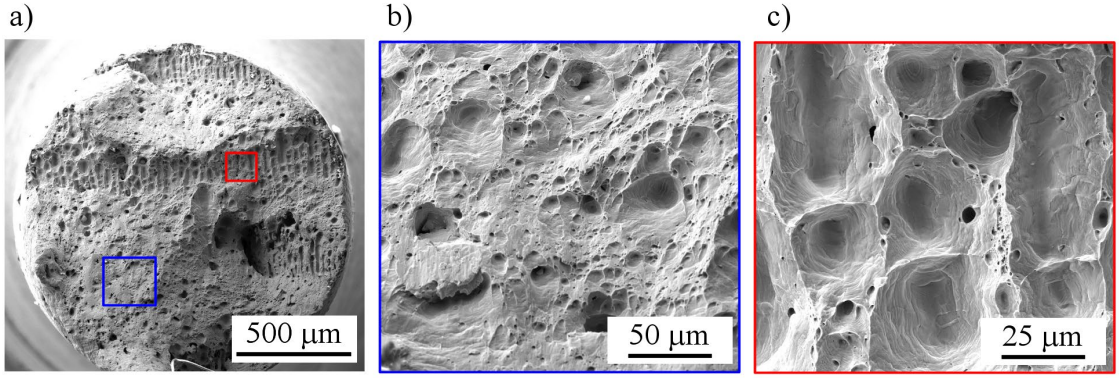

Fig. 5 Detail of fracture surface of tensile specimens for LPBF variant at RT. Overview of fracture surface (a) ductile dimples (b) and details of gas porosity (c).

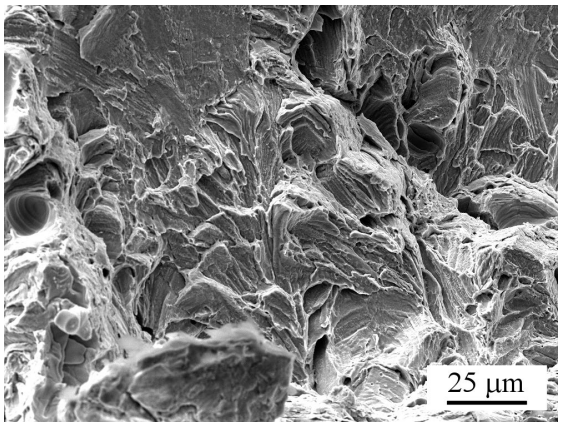

Fig. 6 Detail „cleavage-like“ facets on the fracture surface of tensile specimens for LPBF variant tested at 550 °C.

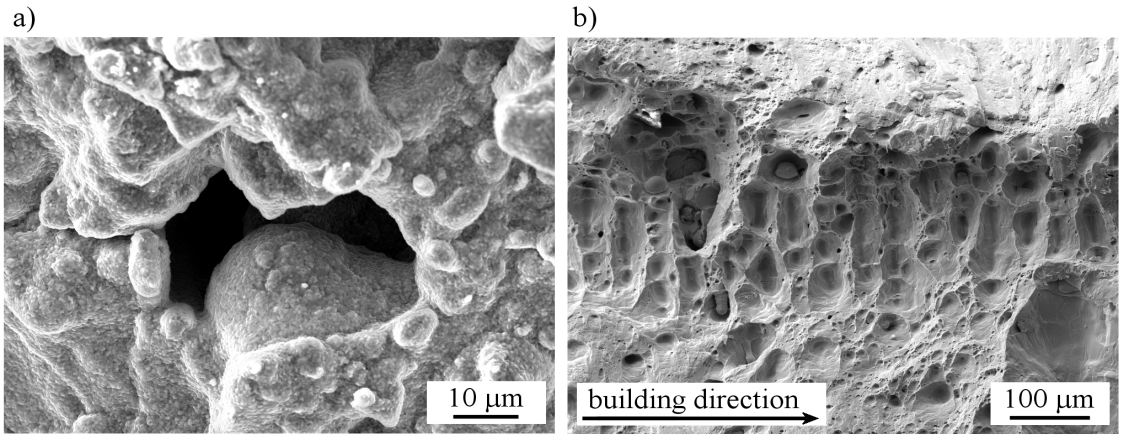

Fig. 7 Defects present in LPBF variant of material: lack-of-fusion pores (a), and keyholes (b).

The occasional presence of LOF was found with small and randomly located defects (see Fig. 7a). LOF defects are related mainly to the lack of the overlap of melt pools respectively laser scan tracks. These defects show highly irregular shapes often partially filled with unmolten powder particles. The balling which is affected by poor wettability was not observed in this work. The most often case of defects in LPBF specimens was spherical gas porosity arranged typically into rows (see Fig. 7b). Generally, the gas porosity can be divided according to the size of pores. Small pores are typically related to the presence of the hydrogen that was bound in the moisture on the surface of the powder particles. Large pores arranged typically in rows in the scanning direction are called keyholes. Keyhole porosity occurs when the power density of the laser beam is high enough to cause metal evaporation. The vapour cavities are locked in the root of the overheated melt pool by solidified

material above it. Keyhole porosity can be distinguished by its usually spherical or elliptical shape elongated in the direction perpendicular to the building direction (see arrow indicating the building direction in Fig. 7b).

Conclusions

Two material variants of Alloy 400 were exposed to the tensile loading at RT and elevated temperatures. Initial microstructure of both cast and LPBF specimens was observed and fractography analysis of fractured specimens was performed. The investigation has resulted in the following conclusions:

1) The LPBF variant shows an increase in yield and ultimate strength but a decrease in plasticity compared to the cast material.

2) The presence of defects (LOF and keyholes) in the LPBF parts results in lowering mechanical properties, especially fracture elongation. Typical and often observed keyhole porosity exhibited elliptical shape, whereas occasionally present lack-of-fusion pores were irregularly shaped. Despite the defects present in the LPBF material which significantly reduce the mechanical properties, very interesting results were achieved.

3) The distribution and type of defects present in LBPF material can provide information about the process conditions. Adjustment of printing parameters will lead to improvement of microstructure quality with a positive effect on the mechanical properties of LBPF material.

Acknowledgement

The authors would like to acknowledge the support of the research project from the European Union's Horizon 2020 research and innovation programme under grant agreement No 958192.

Alice Chlupová would like to acknowledge the support of publication by H2020-WIDESPREAD-2018-03 under grant agreement No. 857124, the Twinning project on the Structural Integrity and Reliability of Advanced Materials obtained through additive Manufacturing (SIRAMM).

References

[1] O. Marenych, A. Kostryzhev, C. Shen, Z. Pan, H. Li, S. van Duin, Precipitation Strengthening in Ni–Cu Alloys Fabricated Using Wire Arc Additive Manufacturing Technology, Metals 9 (1) (2019) 105.

[2] Monel 400. (https://www.hpalloy.com/Alloys/descriptions/MONEL400).

[3] O. Marenych, A. Kostryzhev, Strengthening mechanisms in nickel-copper alloys: A review, Metals 10 (10) (2020) 1358.

[4] K. S. Prakash, T. Nancharaih, V. V. S. Rao, Additive Manufacturing Techniques in Manufacturing -An Overview, Materials Today: Proceedings 5 (2, Part 1) (2018) 3873-3882.

[5] I. Šulák; T. Babinský; A. Chlupová; A. Milovanović; L. Náhlík, Effect of building direction and heat treatment on mechanical properties of Inconel 939 prepared by additive manufacturing, Journal of Mechanical Science and Technology (2022) (accepted for publication)

[6] Y. Shi, Z. Lu, L. Yu, R. Xie, Y. Ren, G. Yang, Microstructure and tensile properties of Zr-containing ODS-FeCrAl alloy fabricated by laser additive manufacturing, Materials Science and Engineering: A 774 (2020) 138937.

[7] I. Raffeis, F. Adjei-Kyeremeh, U. Vroomen, E. Westhoff, S. Bremen, A. Hohoi, A. Bührig-Polaczek, Qualification of a Ni–Cu Alloy for the Laser Powder Bed Fusion Process (LPBF): Its Microstructure and Mechanical Properties, Applied Sciences 10 (10) (2020) 3401.

[8] N. Nudelis, P. Mayr, A Novel Classification Method for Pores in Laser Powder Bed Fusion, Metals 11 (12) (2021) 1912.